SUPPLEMENTAL INFORMATION

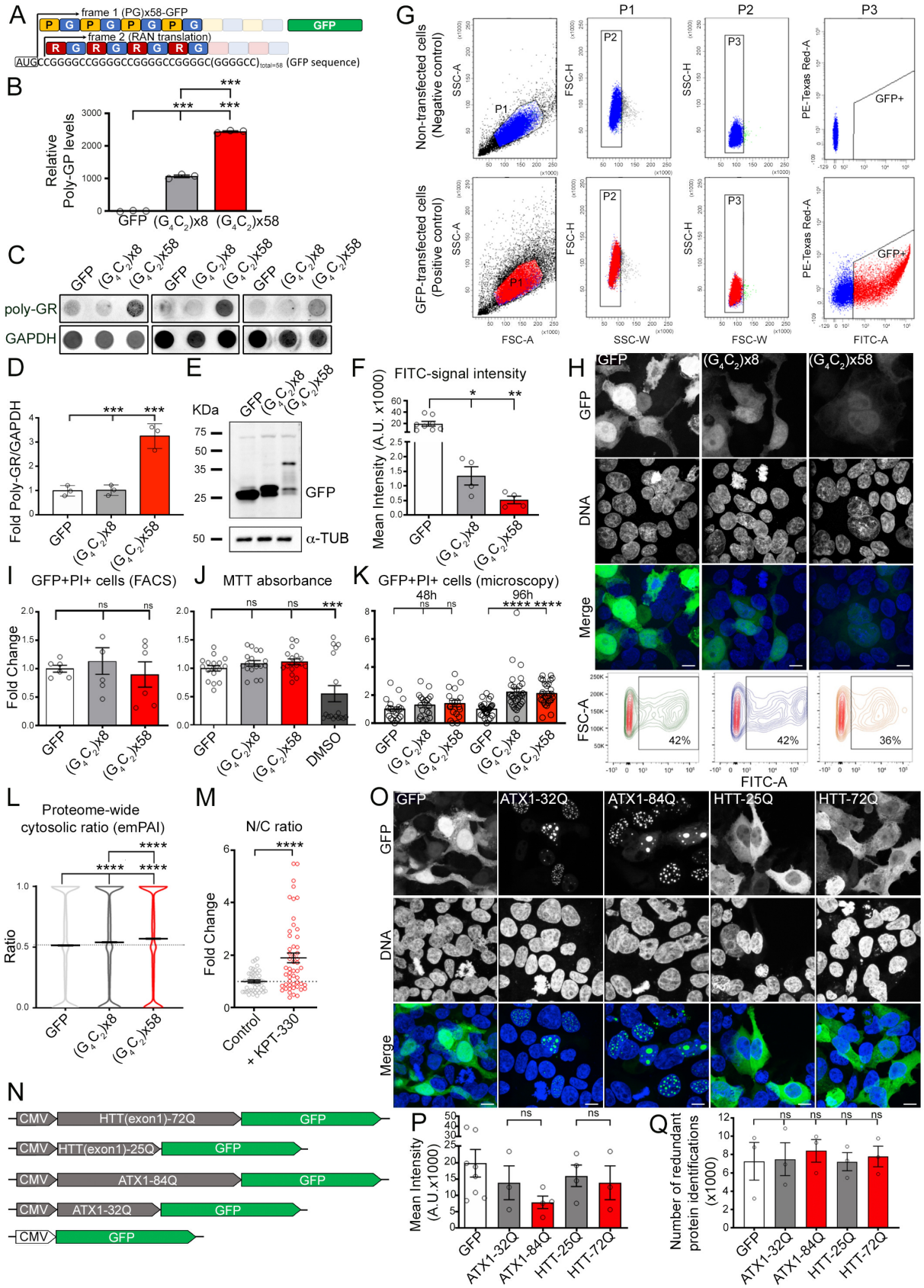

Figure S1, related to Figure 1. Unbiased Proteomic Analysis of Repeat Expansion Mutations Associated With Neurodegeneration.

(A) Schematic showing distinct types of DPRs produced by the C9x58-GFP construct and analyzed in this study.

(B) Bar plots representing the average levels of GP DPR detected by ELISA in cells transfected with GFP, C9x8-GFP, or C9x58-GFP. Individual samples are represented as dots (n=3 independent biological replicates; bars represent mean ± SEM; ANOVA, p***<0.001).

(C) Dot blot of poly-GR in GFP-, C9x8- or C9x58-expressing cells.

(D) Bar plots representing the average levels of poly-GR in cells expressing GFP, C9x8-GFP, and C9x58-GFP. Individual samples are represented as dots (n=3 independent biological replicates; bars represent mean ± SEM; ANOVA, p ***<0.001).

(E) Western blot analysis for GFP in HEK-293 cells transfected with GFP, C9x8-GFP or C9x58-GFP. α-TUBULIN was used as a loading control.

(F) Bar plots displaying the GFP fluorescence levels acquired by FACS analysis in GFP-, C9x8-GFP- or C9x58-GFP-transfected cells. Individual samples are represented as dots (n=4-7 independent biological replicates; bars represent mean ± SEM; ANOVA, p*<0.05, **<0.01).

(G) Representative gating strategy utilized to FACS-purify GFP+ cells.

(H) Top: Representative confocal images of HEK-293 cells transfected with GFP, C9x8-GFP, or C9x58-GFP. Scale bars: 20 μm. Bottom: Representative FACS plots depicting effective percentage of sorted GFP+ cells.

(I) Bar plots displaying FACS-based quantification of double GFP/Propidium Iodide+ cells from HEK-293 cell cultures 48hrs after transfection with GFP, C9x8-GFP or C9x58-GFP. Individual samples are represented as dots (n=2 independent biological replicates; bars represent mean ± SEM; ANOVA, p=ns, not significant).

(J) Bar plots displaying MTT viability assay in HEK-293 cell cultures 48hrs after transfection with GFP, C9x8-GFP or C9x58-GFP. DMSO was used as a positive control. Individual samples are represented as dots (n=3 independent biological replicates; bars represent mean ± SEM; ANOVA, p =ns, not significant, ***<0.001).

(K) Bar plots showing percentage of GFP/Propidium Iodide+ cells counted from images of HEK-293 cells 48 and 96hrs after transfection with GFP, C9x8-GFP or C9x58-GFP. Counted fields are displayed as dots (n=3 independent biological replicates; bars represent mean ± SEM; ANOVA, p=ns, not significant, ****>0.0001).

(L) Violin plots showing the proteome-wide cytosolic ratios calculated by emPAI values of the ~10,000 proteins identified in cells expressing GFP (0.516±0.002; mean ± SEM), C9x8-GFP (0.541±0.002), or C9x58-GFP (0.570±0.002) (n=4 independent biological replicates; bars represent mean ± SEM of proteome-wide cytosolic ratio and the dotted line marks the GFP-transfected cells mean value; Kruskal-Wallis test, p****<0.0001).

(M) Dot plots displaying the fold change in the N/C ratio of the tdTomato reporter in HEK-293 cells treated with the nuclear export inhibitor KPT-330. Individual cells are represented as dots and the dotted line marks the mean N/C ratio in control samples (n=3 independent biological replicates; bars represent mean ± SEM; Mann-Whitney U test, p****<0.0001).

(N) Schematic of the polyglutamine (CAG, polyQ) expansion in *ATX1* or *HTT* (exon 1) used in a comparative subcellular screening of different repeat expansion mutation models.
(O) Representative confocal images of HEK-293 cells transfected with GFP, ATX1-32Q, ATX1-84Q, HTT-25Q, or HTT-72Q. Scale bars: 20 μm.
(P) Bar plots displaying the mean intensity levels of GFP acquired by FACS analysis in GFP-, ATX1-32Q-, ATX1-84Q-, HTT-25Q-, or HTT-72Q-expressing cells. Individual experimental samples are displayed as dots (n=3-7 independent biological replicates; ANOVA, p=ns, not significant).
Q) Bar plots representing the average number of proteins detected in cells expressing GFP, ATX1-32Q, ATX1-84Q, HTT-25Q, or HTT-72Q. Individual experimental samples are displayed as dots (n=3 independent biological replicates; data are represented as mean ± SEM; ANOVA, p=ns, not significant).

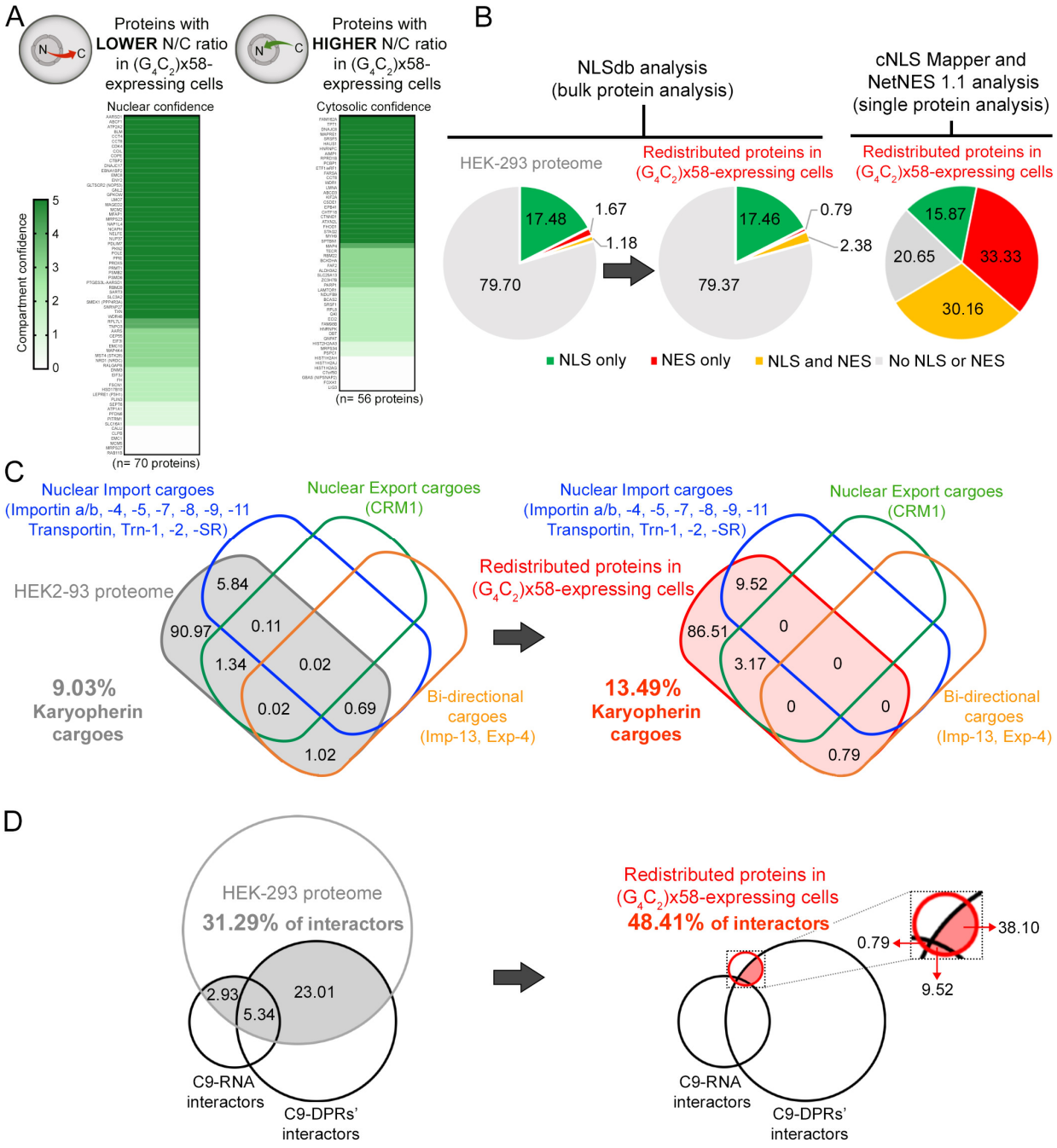
A
Proteins with LOWER N/C ratio in (G4C2)x58-expressing cells
Proteins with HIGHER N/C ratio in (G4C2)x58-expressing cells
Nuclear confidence
Cytosolic confidence
Compartment confidence
5
4
3
2
1
0
(n= 70 proteins)
(n= 56 proteins)
B
NLSdb analysis (bulk protein analysis)
cNLS Mapper and NetNES 1.1 analysis (single protein analysis)
HEK-293 proteome
Redistributed proteins in (G4C2)x58-expressing cells
Redistributed proteins in (G4C2)x58-expressing cells
17.48
1.67
1.18
79.70
17.46
0.79
2.38
79.37
15.87
33.33
20.65
30.16
NLS only
NES only
NLS and NES
No NLS or NES
C
Nuclear Import cargoes (Importin a/b, -4, -5, -7, -8, -9, -11 Transportin, Trn-1, -2, -SR)
Nuclear Export cargoes (CRM1)
HEK2-93 proteome
5.84
90.97
0.11
1.34
0.02
0.02
0.69
1.02
9.03% Karyopherin cargoes
Bi-directional cargoes (Imp-13, Exp-4)
Redistributed proteins in (G4C2)x58-expressing cells
Nuclear Import cargoes (Importin a/b, -4, -5, -7, -8, -9, -11 Transportin, Trn-1, -2, -SR)
Nuclear Export cargoes (CRM1)
9.52
86.51
0
3.17
0
0
0
0.79
13.49% Karyopherin cargoes
Bi-directional cargoes (Imp-13, Exp-4)
D
HEK-293 proteome
31.29% of interactors
2.93
5.34
23.01
C9-RNA interactors
C9-DPRs' interactors
Redistributed proteins in (G4C2)x58-expressing cells
48.41% of interactors
0.79
38.10
9.52
C9-RNA interactors
C9-DPRs' interactors

Figure S2, related to Figure 2. Analysis of Subcellular Proteomic Changes Identified in Cells Carrying the C9-HRE.

(A) Heat maps representing the subcellular protein localization analysis of proteins enriched in the cytosol (left) or in the nucleus (right) of C9x58-expressing cells. The presence of these proteins in the nucleus or the cytosol is ranked based on confidence values established by the https://compartments.jensenlab.org database. Color code legend on the left indicates the probability of proteins to be absent (Confidence=0, white) or present (Confidence=1 to 5, from light to dark green) in the nucleus (left) or in the cytosol (right).

(B) Pie charts representing the percentage of proteins of the global HEK-293 proteome (left chart) and of the redistributed proteins in C9x58-expressing cells (middle chart) that contain both NLS and NES (yellow), NLS only (green), NES only (red), or neither of these sequences (gray), based on NLSdb analysis. Right pie chart showing the resultant cNLS Mapper and NetNES 1.1 analysis of nuclear localization sequences in the group of redistributed proteins observed in C9x58-expressing cells.

(C) Venn diagrams displaying the overlap of previously published nuclear import, export and bi-directional karyopherin cargoes with the HEK-293 proteome (left) or with the group of redistributed proteins in C9x58-expressing cells (right).

(D) Venn diagrams displaying the overlap between previously reported C9-HRE-RNA and C9-HRE DPR protein interactors, with the HEK-293 proteome (left) or with the group of redistributed proteins in C9x58-expressing cells (right).

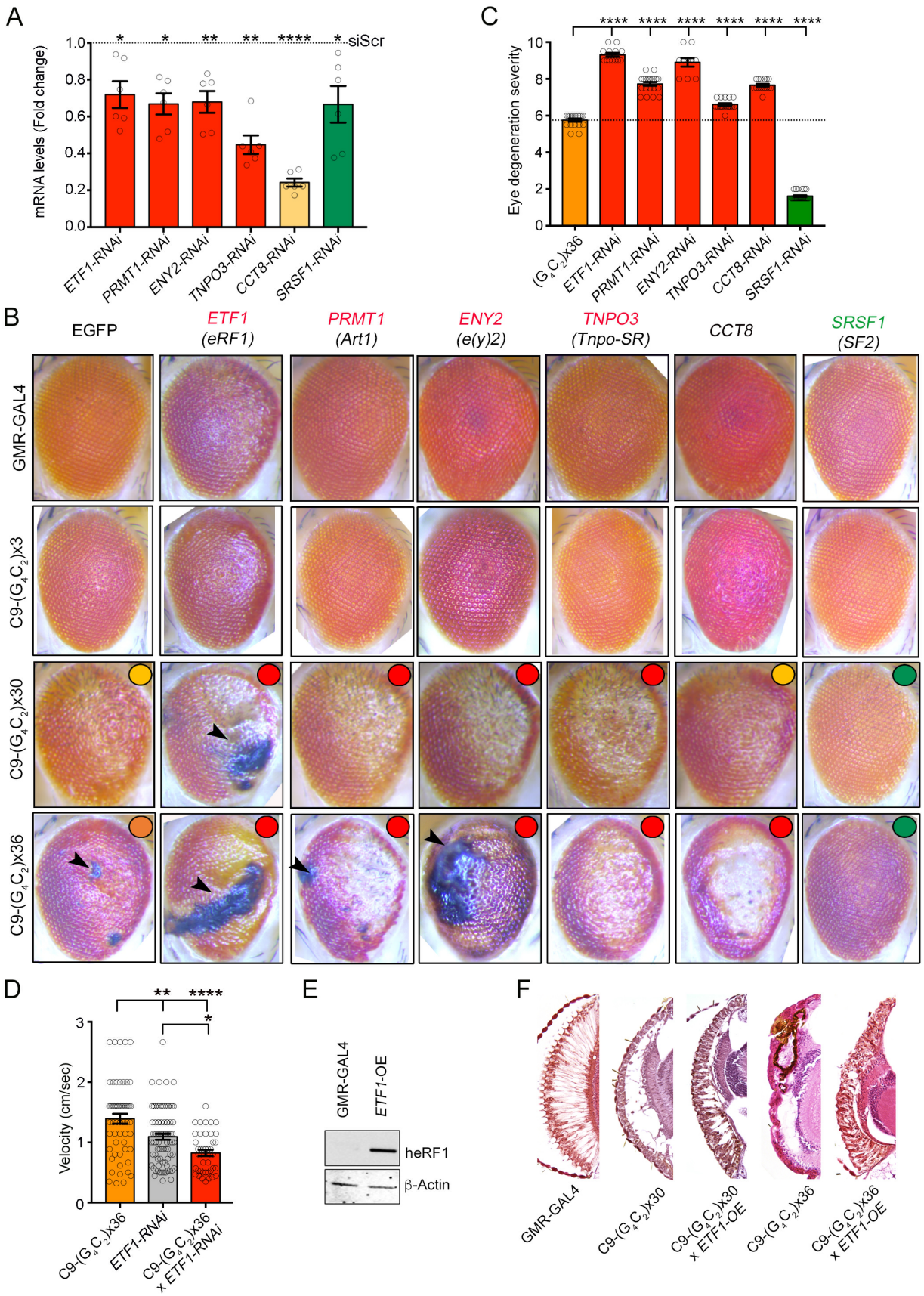
A
mRNA levels (Fold change)
siScr
ETF1-RNAi
PRMT1-RNAi
ENY2-RNAi
TNPO3-RNAi
CCT8-RNAi
SRSF1-RNAi
C
Eye degeneration severity
(G4C2)x36
B
EGFP
ETF1 (eRF1)
PRMT1 (Art1)
ENY2 (e(y)2)
TNPO3 (Tnpo-SR)
CCT8
SRSF1 (SF2)
GMR-GAL4
C9-(G4C2)x3
C9-(G4C2)x30
C9-(G4C2)x36
D
Velocity (cm/sec)
C9-(G4C2)x36 x ETF1-RNAi
E
GMR-GAL4
ETF1-OE
heRF1
β-Actin
F
C9-(G4C2)x30 x ETF1-OE
C9-(G4C2)x36 x ETF1-OE

Figure S3, related to Figure 3. Representative Redistributed Proteins are Genetic Modifiers of *C9orf72* Repeat Expansion Toxicity in *Drosophila* Disease Models.

(A) Bar plots displaying RT-qPCR results of target genes in RNAi *Drosophila* models. Individual flies are displayed as dots and dashed line marks the respective mean levels in control flies (n=6 flies; bars represent mean ± SEM; Mann-Whitney U test, p*<0.05, **<0.01, ****<0.0001).

(B) Representative eye images of the different C9-ALS flies (C9x30 and x36), and controls (GMR-GAL4 and C9x3) crossed with the multiple knockdown flies tested (*ETF1*, *PRMT1*, *ENY2*, *TNPO3*, *CCT8*, *SRSF1*; homologous gene names in Drosophila are displayed in parenthesis if different). Colored circles on the top right of eye images of C9-ALS flies crossed with the multiple knockdown flies indicate the eye degeneration change on quantifications shown in C: C9x30 toxic level is shown in yellow; C9x36 toxic level is shown in orange; suppression and enhancement of C9-HRE toxicity are shown in green and red, respectively.

(C) Bar plots displaying the level of eye degeneration in flies carrying the C9x36 repeats with RNAi for *ETF1*, *PRMT1*, *ENY2*, *TNPO3*, *CCT8*, or *SRSF1*. Enhancers and suppressors of toxicity are represented by red and green bars, respectively. The basal level of eye degeneration in C9x36 flies is shown in orange. Individual flies are represented as dots and the dotted line marks the mean level of eye degeneration in RNAi control C9x36 repeat flies (n ≥10 flies; bars represent mean ± SEM; Mann-Whitney U test, p****<0.0001).

(D) Bar plots displaying climbing velocity in C9x36, *ETF1*-RNAi and C9x36 x *ETF1*-RNAi flies. Individual flies are displayed as dots (n ≥43 flies; bars represent mean ± SEM; ANOVA, p*<0.05, **<0.01, ****<0.0001).

(E) Western blot analysis for human eRF1 expression in control (GMR-GAL4) and *ETF1*-OE flies. β-Actin was used as a loading control.

(F) Transverse eye sections showing the level of degeneration in C9-HRE flies (C9x30 and x36) with respect to control (GMR-GAL4) and eRF1 overexpression [(C9x30 x *ETF1*-OE) and (C9x36 x *ETF1*-OE)] flies.

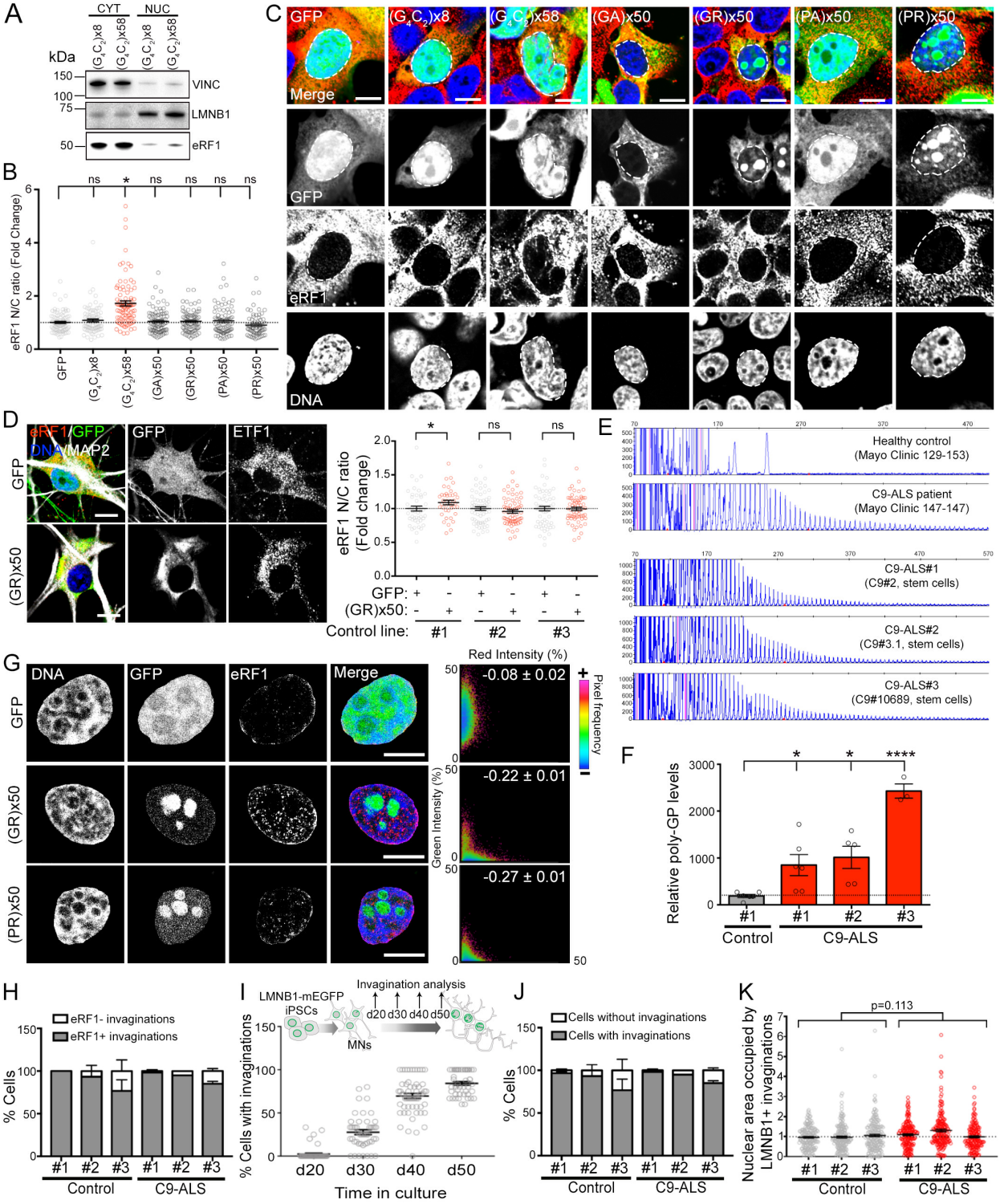
A
CYT
NUC
kDa
(G4C2)x8
(G4C2)x58
150
100
75
50
VINC
LMNB1
eRF1
B
eRF1 N/C ratio (Fold Change)
ns
*
GFP
(G4C2)x8
(G4C2)x58
(GA)x50
(GR)x50
(PA)x50
(PR)x50
C
GFP
Merge
eRF1
DNA
D
eRF1/GFP
DNA/MAP2
ETF1
eRF1 N/C ratio (Fold change)
GFP: + - + - + -
(GR)x50: - + - + - +
Control line: #1 #2 #3
E
Healthy control (Mayo Clinic 129-153)
C9-ALS patient (Mayo Clinic 147-147)
C9-ALS#1 (C9#2, stem cells)
C9-ALS#2 (C9#3.1, stem cells)
C9-ALS#3 (C9#10689, stem cells)
F
Relative poly-GP levels
****
Control
C9-ALS
G
DNA
GFP
eRF1
Merge
Red Intensity (%)
Green Intensity (%)
Pixel frequency
-0.08 ± 0.02
-0.22 ± 0.01
-0.27 ± 0.01
H
eRF1- invaginations
eRF1+ invaginations
% Cells
I
LMNB1-mEGFP
iPSCs
MNs
Invaginations analysis
d20 d30 d40 d50
% Cells with invaginations
Time in culture
J
Cells without invaginations
Cells with invaginations
K
p=0.113
Nuclear area occupied by LMNB1+ invaginations

Figure S4, related to Figure 4. eRF1 is Redistributed in *C9orf72* iPSC-Derived Motor Neurons.

(A) Representative western blot bands for eRF1 levels in the nuclear and cytosolic fractions of cells expressing C9x8-GFP and C9x58-GFP. VINCULIN and LMNB1 were used as cytosolic and nuclear markers, respectively.

(B) Dot plot displaying the fold change in the N/C ratio of eRF1 signal quantified in HEK-293 cells expressing GFP, C9x8-, C9x58-, (GA)x50-, (GR)x50-, (PA)x50- or (PR)x50-GFP. Individual cells are displayed as dots and dotted line marks the mean eRF1 N/C ratio in control GFP-expressing cells (n=3 independent biological replicates; bars represent mean ± SEM; Kruskal-Wallis test; p =ns, not significant, *<0.05).

(C) Confocal images of GFP, C9x8-, C9x58-, (GA)x50-, (GR)x50-, (PA)x50- or (PR)x50-GFP transfected cells immunolabeled for eRF1 (red) and DNA (blue). Dashed line marks the nuclear boundary. Scale bars: 10 μm.

(D) Left: Representative confocal images of healthy control MNs infected with GFP (top panel), or (GR)x50-GFP (bottom panel) and immunolabeled for eRF1 (red), MAP2 (white), and DNA (blue). Scale bars: 10 μm. Right: Dot plot showing the fold change in the N/C ratio of eRF1 signal in MNs derived from 3 healthy control iPSC lines infected with GFP or (GR)x50-GFP. Individual cells are displayed as dots and dotted line marks the mean N/C ratio of eRF1 signal in GFP-infected iPSC-derived MNs (n=2-3 independent differentiations; bars represent mean ± SEM; Mann-Whitney U test, p=ns, not significant, *<0.05).

(E) Repeat primed PCR analysis on 3 C9-ALS patient iPSC lines utilized in this study. Healthy control, and C9-ALS patient samples (top) were utilized as a negative and positive control, respectively.

(F) Bar plots showing the poly-GP levels detected by ELISA in 1 control and 3 C9-ALS iPSC-derived MNs. Individual samples are represented as dots and the dotted line marks the mean levels of poly-GP in control iPSC-derived MNs (n=3-5 independent differentiations; bars represent the mean ± SEM; ANOVA, p*<0.05; ****<0.0001).

(G) Left: Representative confocal images of HEK-293 nuclei expressing GFP, (GR)x50- or (PR)x50-GFP (green), and immunolabeled for eRF1 (red) and DNA (blue). Scale bars: 5 μm. Right: Scatter plots where each point reflects the DPR-GFP (green) signal intensity on the y-axis, and eRF1 signal intensity (red) on the x-axis. The mean ± SEM of the Pearson's correlation coefficient for the entire dataset is displayed within the corresponding plot.

(H) Bar plot showing the percentage of controls and C9-ALS iPSC-derived MNs that contain nuclear invaginations with (gray bars) or without (white bars) eRF1.

(I) Top: Schematic illustrating the time course analysis of nuclear invaginations in LMNB1-mEGFP iPSC-derived MNs carried out. Bottom: Dot plot displaying the percentage of LMNB1-mEGFP iPSC-derived MNs containing nuclear invaginations at day 20, 30, 40 and 50 of MN differentiation.

(J) Bar plot showing the percentage of controls and C9-ALS iPSC-derived MNs with (gray bars) or without (white bars) nuclear invaginations at day 50 of differentiation.

(K) Dot plot displaying the fold change of the nuclear area occupied by nuclear invaginations in MNs derived from 3 controls and 3 C9-ALS patient iPSC lines. Individual cells are represented as dots and the dotted line marks the mean occupied area in control

samples (n=3 independent differentiations; bars represent mean ± SEM; Mann-Whitney U test, p=0.113).

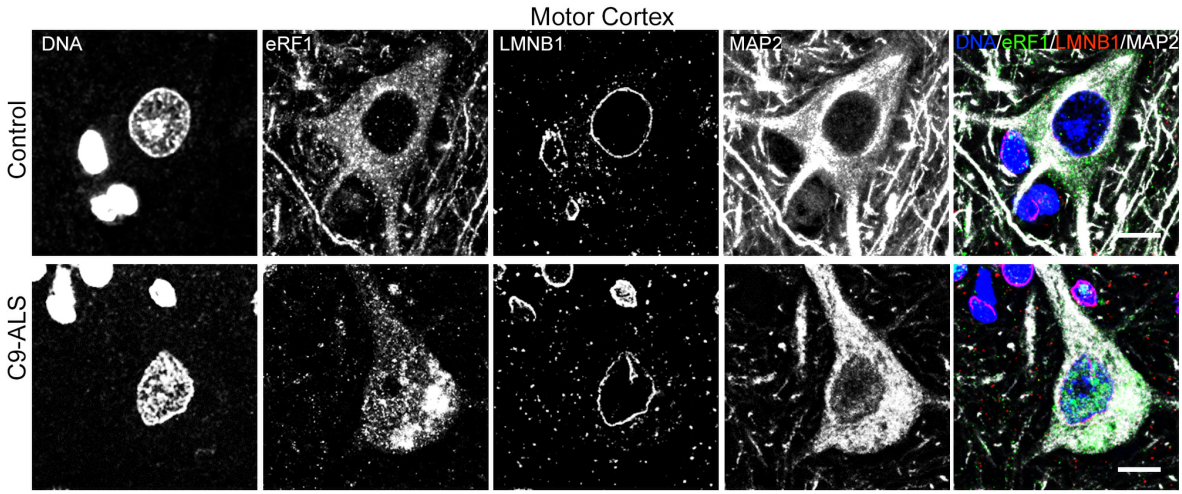

Figure S5, related to Figure 5. eRF1 Accumulates in Neuronal Nuclei of *C9orf72* ALS Patients Postmortem Tissue. Representative IHC confocal images of layer V neurons immunolabeled for eRF1 (green), LMNB1(red), MAP2 (white), and DNA (blue) in motor cortex tissue from a non-neurological control and a C9-ALS patient. Scale bars: 10μm.

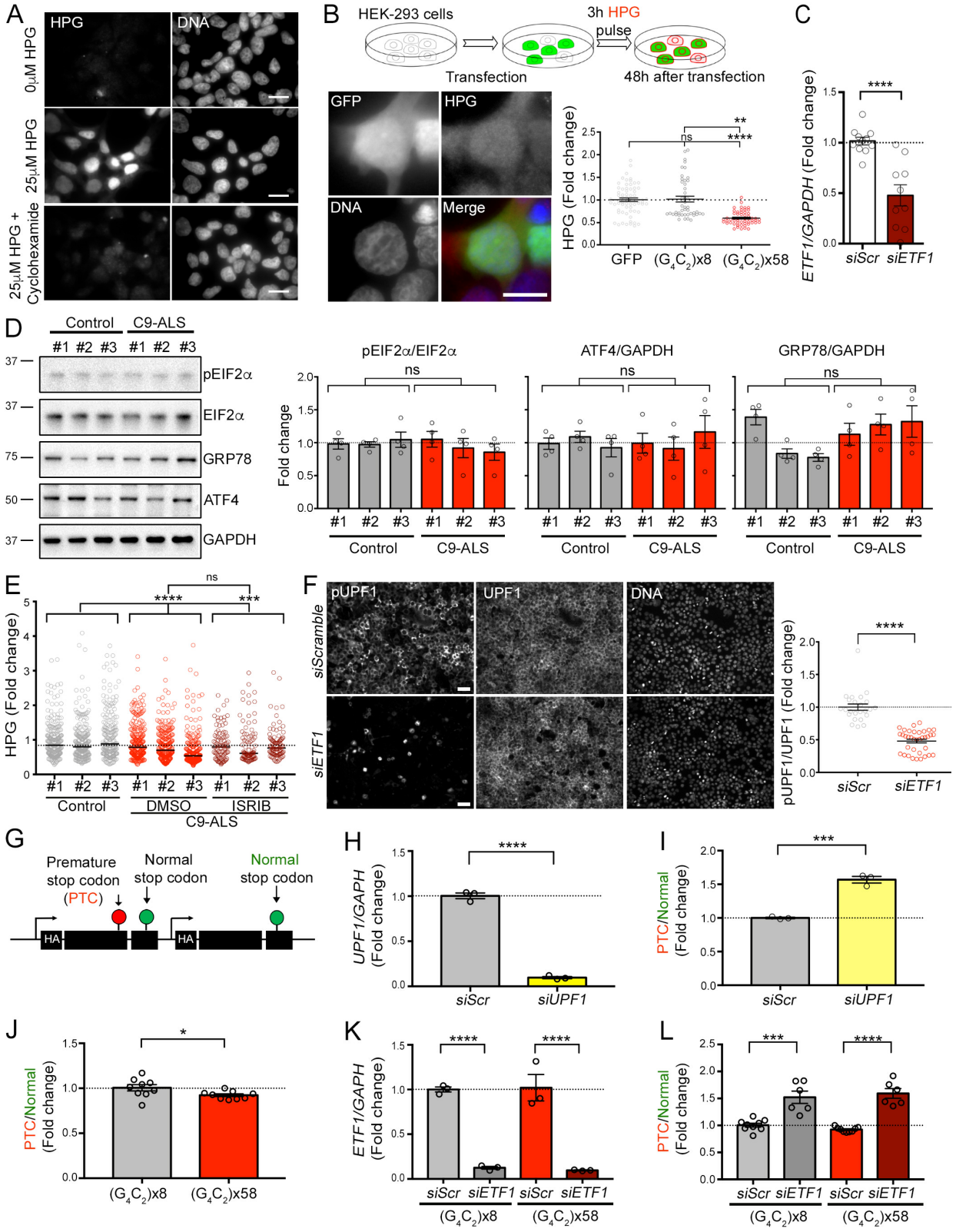
A
HPG
DNA
0μM HPG
25μM HPG
25μM HPG + Cycloheximide
B
HEK-293 cells
3h HPG pulse
Transfection
48h after transfection
GFP
HPG
DNA
Merge
HPG (Fold change)
ns
**
****
GFP
(G4C2)x8
(G4C2)x58
C
ETF1/GAPDH (Fold change)
****
siScr
siETF1
D
Control
C9-ALS
#1 #2 #3 #1 #2 #3
pEIF2α
EIF2α
GRP78
ATF4
GAPDH
pEIF2α/EIF2α
ATF4/GAPDH
GRP78/GAPDH
Fold change
ns
Control
C9-ALS
E
HPG (Fold change)
ns
****
***
Control
DMSO
ISRIB
C9-ALS
F
pUPF1
UPF1
DNA
siScramble
siETF1
pUPF1/UPF1 (Fold change)
****
siScr
siETF1
G
Premature stop codon (PTC)
Normal stop codon
Normal stop codon
HA
HA
H
UPF1/GAPH (Fold change)
****
siScr
siUPF1
I
PTC/Normal (Fold change)
***
siScr
siUPF1
J
PTC/Normal (Fold change)
*
(G4C2)x8
(G4C2)x58
K
ETF1/GAPH (Fold change)
****
****
siScr
siETF1
siScr
siETF1
(G4C2)x8
(G4C2)x58
L
PTC/Normal (Fold change)
***
****
siScr
siETF1
siScr
siETF1
(G4C2)x8
(G4C2)x58

Figure S6, related to Figure 6. eRF1 is a Key Regulator of Protein Translation and NMD.

(A) Quality control analysis of the Click-iT HPG method utilized to measure *de novo* protein translation. Representative images of HEK-293 cells labeled for HPG incorporation and DNA, showing differential fluorescence intensity between cells treated with 25 μM HPG (middle) and untreated cells (top), or cells treated with the translation inhibitor cycloheximide (CHX; bottom). Scale bars: 20μm.

(B) Top: Schematic of *de novo* protein translation assay performed in transfected HEK-293 cells. Bottom left: Representative image of Click-iT HPG fluorescent labeling of *de novo* protein synthesis in GFP-expressing cells. Scale bar: 20 μm. Bottom right: dot plot displaying the levels of *de novo* protein translation assessed by HPG incorporation in GFP-, C9x8- and C9x58-expressing cells. Individual cells are represented as dots and the dotted line marks the mean level in the GFP control condition (n=3 independent biological replicates; bars represent mean ± SEM; Kruskal-Wallis test, p=ns, not significant, **<0.01, ****<0.0001).

(C) Dot plot showing the *ETF1* mRNA levels, analyzed by qPCR, in control and C9-ALS iPSC-derived MNs transfected with scrambled or *ETF1* siRNA. *GAPDH* was used as housekeeping gene. Individual samples are represented as dots and the dotted line marks the mean *ETF1* expression levels in siScr-transfected MNs (n=3 independent differentiation; bars represent mean ± SEM; T test, p****<0.0001).

(D) Left: Representative western blot analysis for ISR markers (pEIF2α, GRP78 and ATF4) in MN cultures derived from 3 control and 3 C9-ALS iPSC lines. EIF2α and GAPDH were used as loading controls. Right: bar plots displaying the fold change in the protein levels of ISR markers in 3 C9-ALS *vs.* 3 healthy control iPSC-derived MNs. Individual samples are displayed as dots and dotted lines mark the mean ratio value in control samples (n=4 independent differentiations; bars represent the mean ± SEM; T test, p=ns, not significant).

(E) Dot plot displaying the fold change of HPG incorporation in MNs derived from 3 controls and 3 C9-ALS patient iPSC lines treated with vehicle (DMSO) or ISR inhibitor (ISRIB). Individual cells are represented as dots and the dotted line marks the mean protein translation in control samples (n=3 independent differentiations; bars represent median; Kruskal-Wallis test; p=ns, not significant, ***<0.001, ****<0.0001).

(F) Left: ICC analysis of NMD activation as measured by the pUPF1/UPF1 ratio upon *ETF1* knockdown in HEK-293 cells. Scale bar: 50 μm. Right: Dot plot showing the pUPF1/UPF1 levels in HEK-293 cells transfected with scramble and *ETF1* siRNAs. Individual analyzed fields are displayed as dots and the dotted line marks the ratio mean in the siScr control condition (n=3 biological replicates; bars represent mean ± SEM; Mann-Whitney U test, p****<0.0001).

(G) Schematic of the reporter construct utilized to assess NMD activity *in vitro*. The construct encodes two TRB (T cell receptor-β) minigenes sharing >99% homology and fused to an HA tag; one of them contains a premature stop codon (PTC) that produces a truncated protein.

(H) Dot plot showing qPCR analysis of *UPF1* mRNA levels in HEK-293 cells transfected with scrambled or *UPF1* siRNA. *GAPDH* was used as housekeeping gene. Individual samples are represented as dots and the dotted line marks the mean *UPF1* expression

levels in siScr-transfected cells (n=3 independent biological replicates; bars represent mean ± SEM; T test, p****<0.0001).
(I) qPCR analysis of the ratio of truncated (PTC) to full-length (normal) RNA products of the TRB minigenes in HEK-293 cells transfected with scrambled or UPF1 siRNAs. Individual samples are represented as dots and the dashed line marks PTC/Normal ratio in siScr-transfected HEK-293 cells (n=3 independent biological replicates; bars represent mean ± SEM; T test, p***<0.001).
(J) Bar plot displaying the quantification of the average NMD activity, calculated by the PTC relative to full-length product in cells expressing C9x8-GFP or C9x58-GFP. Independent replicates are displayed as dots and dotted line marks the mean PTC/normal ratio in control samples (n=3 independent biological replicates; bars represent mean ± SEM; T test, p*<0.05).
(K) Dot plot depicting the RT-qPCR analysis of *ETF1* mRNA levels in C9x8- and C9x58-expressing cells co-transfected with scrambled or *ETF1* siRNA. *GAPDH* was used as housekeeping gene. Independent replicates are displayed as dots and dotted line marks the mean *ETF1* levels in siScr-transfected HEK-293 cells (n=3 independent biological replicates; bars represent mean ± SEM; T test, p****<0.0001).
(L) Dot plot displaying the quantification of NMD activity by qPCR in HEK-293 cells expressing C9x8-GFP and C9x58-GFP with normal or reduced levels of *ETF1*. Individual samples are displayed as dots and dotted line marks the mean PTC/normal ratio in siScr-C9x8-transfected cells (n=2 biological replicates; horizontal bars represent mean ± SEM; ANOVA, p***<0.001, ****<0.0001).

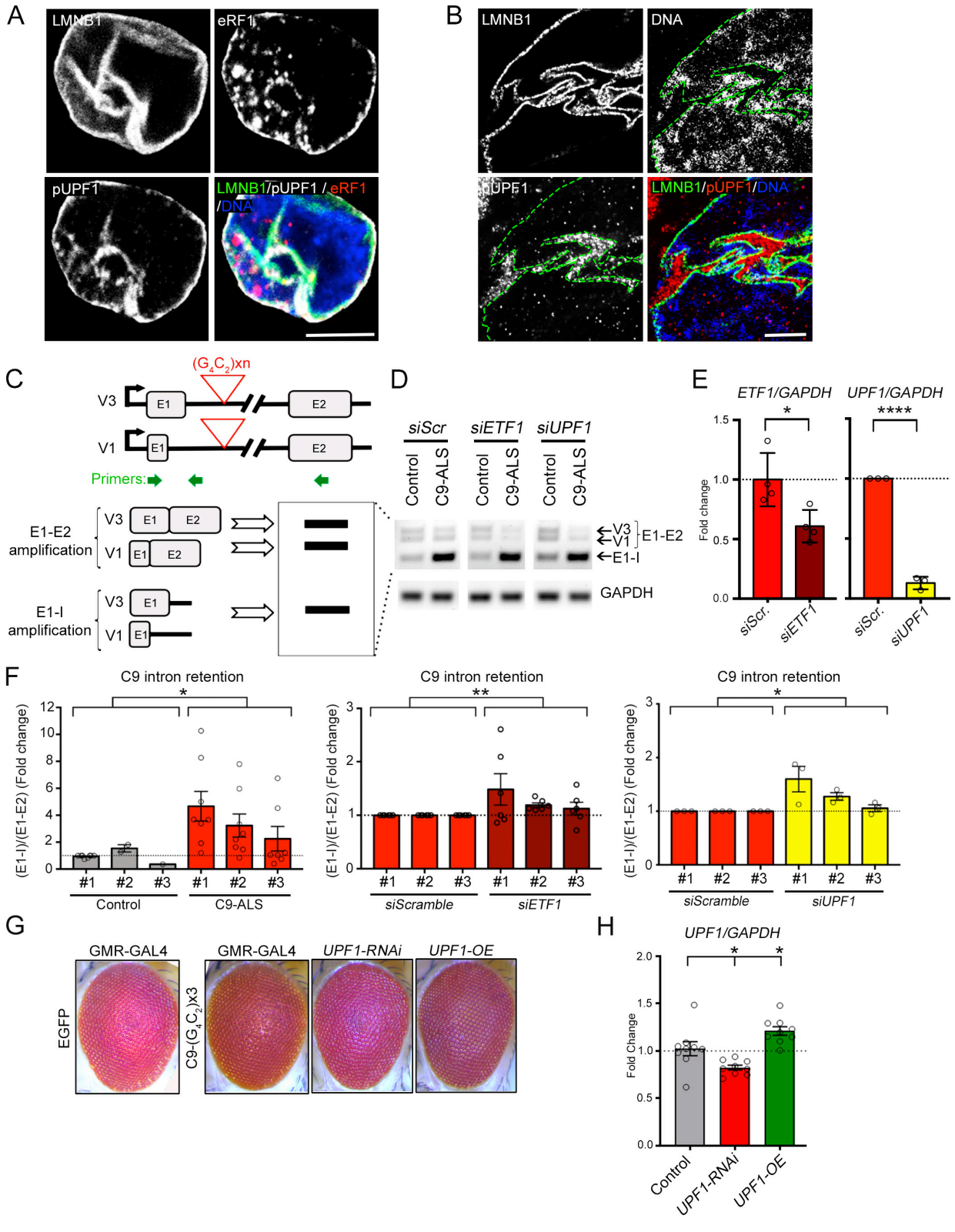
A
LMNB1
eRF1
pUPF1
LMNB1/pUPF1 / eRF1 /DNA
B
LMNB1
DNA
pUPF1
LMNB1/pUPF1/DNA
C
(G4C2)xn
V3
V1
E1
E2
Primers:
E1-E2 amplification
E1-I amplification
D
siScr
siETF1
siUPF1
Control
C9-ALS
V3
V1
E1-E2
E1-I
GAPDH
E
ETF1/GAPDH
UPF1/GAPDH
Fold change
siScr.
siETF1
siUPF1
F
C9 intron retention
(E1-I)/(E1-E2) (Fold change)
Control
C9-ALS
siScramble
siETF1
siScramble
siUPF1
G
GMR-GAL4
GMR-GAL4
UPF1-RNAi
UPF1-OE
EGFP
C9-(G4C2)x3
H
UPF1/GAPDH
Fold Change
Control
UPF1-RNAi
UPF1-OE

Figure S7, related to Figure 7: NMD Targets the Expanded *C9orf72* Transcript.
(A) Representative confocal image of an iPSC-derived MN nucleus labeled for eRF1 (red), pUPF1 (white), LMNB1 (green), and DNA (blue), showing high degree of colocalization between eRF1 and pUPF1 within LMNB1+ nuclear invaginations. Scale bar: 5 μm.
(B) Representative expansion microscopy image of a C9-ALS patient MN nucleus immunolabeled for LMNB1 (green), pUPF1 (red), and DNA (blue), showing the accumulation of pUPF1 (red) on the cytosolic side of nuclear invaginations. Dashed lines indicate the nuclear envelope border. Scale bar: 10 μm.
(C) Schematic of the C9 intron retention assay utilized in this study.
(D) RT-PCR-based C9 intron retention analysis, by comparing the ratio of the mutant (E1-I) relative to wild type (E1-E2) transcript in 1 control and 3 C9-ALS patient-derived MNs treated with scramble, *ETF1*, or *UPF1* siRNAs. Control and C9-ALS adjacent bands for each transfected condition, from the same gel and acquisition time exposure, were cropped to display representative changes observed in the multiple tested conditions.
(E) Bar plots showing qPCR analysis of *ETF1* (left) and UPF1 (right) mRNA levels in C9-ALS iPSC-derived MNs transfected with scrambled and *ETF1* or *UPF1* siRNAs, respectively. *GAPDH* was used as housekeeping gene. Individual samples are represented as dots and the dotted line marks basal levels of *ETF1* and *UPF1* in siScr-C9-ALS iPSC-derived MNs (n=4, left graph, and n=3, right graph independent differentiations; data are represented the mean ± SEM; T test, p*<0.05, ****<0.0001).
(F) Bar plots showing fold change levels of C9-intron retention, as measured by RT-PCR, obtained from MN cultures derived from 3 control and 3 C9-ALS iPSC lines (left graph), in C9-ALS iPSC-derived MNs transfected with scrambled (Scr) *vs. ETF1* siRNAs (middle graph), and in C9-ALS iPSC-derived MNs transfected with Scr *vs. UPF1* siRNAs (right graph). Individual samples are displayed as dots and dotted line marks the mean C9 intron retention in controls (left graph) and in siScr-transfected C9-ALS (middle and right graphs) MNs (n=8 (left), 6 (middle), 3 (right) independent differentiations; bars represent the mean ± SEM; Mann-Whitney (left and right graphs), and t test (middle graph), p*<0.05; ***<0.01).
(G) Representative images of fly eyes from wild-type (GMR-GAL4 x EGFP) or C9x3 control mutant flies, with endogenous levels (EGFP), knockdown (*UPF1*-RNAi) or overexpression (*UPF1*-OE) of UPF1.
(H) Dot plot showing qPCR analysis of *UPF1* mRNA levels in the Drosophila models of *UPF1* knockdown (*UPF1*-RNAi) and overexpression (*UPF1*-OE). *GAPDH* was used as housekeeping gene. Individual flies are represented as dots and the dotted line marks the mean *UPF1* levels in control flies (n=9 flies/condition; bars represent mean ± SEM; ANOVA, p *<0.05).